Phase equilibria in polydisperse colloidal systems

Moreno Fasolo, Peter Sollich, Alessandro Speranza
Department of Mathematics, King's College London,
Strand, London WC2R 2LS, U.K. Email: peter.sollich@kcl.ac.uk

October 10, 2003

Abstract

Many materials containing colloids or polymers are polydisperse: they comprise particles with properties (such as diameter, charge, or polymer chain length) that depend continuously on one or several parameters. This effectively infinite number of distinguishable particle species makes the theoretical prediction of phase equilibria a highly nontrivial task. We give an overview of recent progress, focussing on the "moment free energy" method which reduces the problem to one involving only the densities of a finite number of quasi-species. Applications to isotropic-nematic phase equilibria of rodlike particles and to the phase behaviour of polydisperse hard spheres are described.

1 Introduction

Statistical mechanics was originally developed for the study of large systems of identical particles such as atoms and small molecules. However, many materials of industrial and commercial importance which contain colloidal particles or polymers do not fit neatly into this framework. For example, the particles in a colloidal suspension are never precisely identical to each other, but have a range of diameters (and/or surface charges, shapes etc): they are *polydisperse*.

In this article we focus on the effects of polydispersity on *phase behaviour*: to process a colloidal or polymeric material, one needs to know under which conditions of pressure and temperature it will be stable against demixing, how many phases will result if it does demix, and what their properties are. The emphasis will be on the problem of predicting such (equilibrium, bulk) phase behaviour theoretically. We outline the recently developed "moment free energy method" [1, 2] and give some recent results for suspensions of rodlike and spherical colloidal particles. We will omit much detail and refer for this, along with a more comprehensive overview of related work and an extensive bibliography, to the recent review [3]; for a more detailed description of the moment free energy method itself the best resource is [4].

2 Polydisperse phase equilibria: the challenge

To understand why the prediction of phase equilibria in polydisperse systems is a challenging problem, recall first the procedure for a monodisperse system. In a suspension of identical colloidal particles the experimentally controlled variables would be temperature T, suspension volume V, and particle number N; the appropriate thermodynamic potential is the Helmholtz free energy $F(N,V,T)$. (Solvent degrees of freedom are assumed to have been eliminated, so that the energetic part of F arises from the potential of mean force.) Phase separation occurs if it lowers the total free energy. Conservation of N and V then lead to the conditions of equality of chemical potential $\mu = \partial F/\partial N$ and (osmotic) pressure $\Pi = -\partial F/\partial V$ between coexisting phases. Since the free energy is extensive, it can be written as $F(N,V,T) = Vf(\rho,T)$ where $\rho = N/V$ is the (number) density of colloids. In terms of the free energy *density* $f(\rho,T)$, one has $\mu = \partial f/\partial\rho$ and $\Pi = -f + \mu\rho$; the latter is just the Gibbs-Duhem relation. Equality of μ and Π then implies that a plot of f vs. ρ has a double tangent at the densities of the two coexisting phases (see *e.g.* [5]). From these densities one can also find the fraction of the system volume $v^{(\alpha)} = V^{(\alpha)}/V$ occupied by each phase α: particle conservation can be written as $\sum_\alpha v^{(\alpha)}\rho^{(\alpha)} = \rho$, and together with $v^{(1)}+v^{(2)} = 1$ gives for two phases the well-known "lever rule" $v^{(1)} = (\rho - \rho^{(2)})/(\rho^{(1)} - \rho^{(2)})$.

Moving towards the polydisperse case, assume now that there are M different species of colloid particles, each with its own particle number N_i and corresponding density $\rho_i = N_i/V$. All densities are conserved, so that

$$\sum_\alpha v^{(\alpha)}\rho_i^{(\alpha)} = \rho_i \tag{1}$$

if the system separates into several phases. The free energy (density) $f(\{\rho_i\})$ is now a function of all M densities, as well as the fixed temperature T which we suppress from now on in the notation. A plot of $f(\{\rho_i\})$ against the densities ρ_i would give a (hyper-) surface in a graph with $M+1$ coordinate axes, and to find phase coexistences we would have to construct multiple tangent (hyper-) planes to this surface. Where such tangent planes exist, the total free energy is lowered by phase separation into the appropriate number of phases (which, from Gibbs' phase rule, can be between two and $M+1$). The densities $\rho_i^{(\alpha)}$ in the different phases are given by the points where the tangent plane touches the free energy surface, and the fractional phase volumes $v^{(\alpha)}$ follow from the conditions (1) together with $\sum_\alpha v^{(\alpha)} = 1$.

Now consider the fully polydisperse case. Let σ be the polydisperse attribute of the particles, *e.g.* the particle diameter in spherical colloids or the chain length in polymers. To fully describe the composition of the system we need a *density distribution* $\rho(\sigma)$, defined such that $\rho(\sigma)d\sigma$ is the density of particles with σ-values in the range $[\sigma, \sigma+d\sigma]$. Formally, this corresponds to a scenario with an infinite number of particle species, as can be seen by splitting the range of σ into M "bins", defining the ρ_i to be the densities within each bin, and then taking $M \to \infty$ (see *e.g.* [6]). The tangent plane procedure for finding phase coexistences then clearly becomes unmanageable, both conceptually and numerically: one would have to work in an infinite-dimensional space—mathematically, the free energy becomes a *functional* $f([\rho(\sigma)])$ of $\rho(\sigma)$—and Gibbs' phase rule allows the coexistence of arbitrarily many thermodynamic phases.

The challenge in predicting polydisperse phase equilibria thus arises from the effectively infinite number of conserved densities, rendering standard approaches developed for mixtures of a finite number of species useless. Notice that the issue here is that of determining the phase equilibria from a free energy (functional) which is assumed *known*. The calculation of this free energy from first principles is a different and no less challenging problem that we will not address here. Accordingly, whenever we refer to "exact" results below, we mean the exact thermodynamics of a model as specified by its free energy.

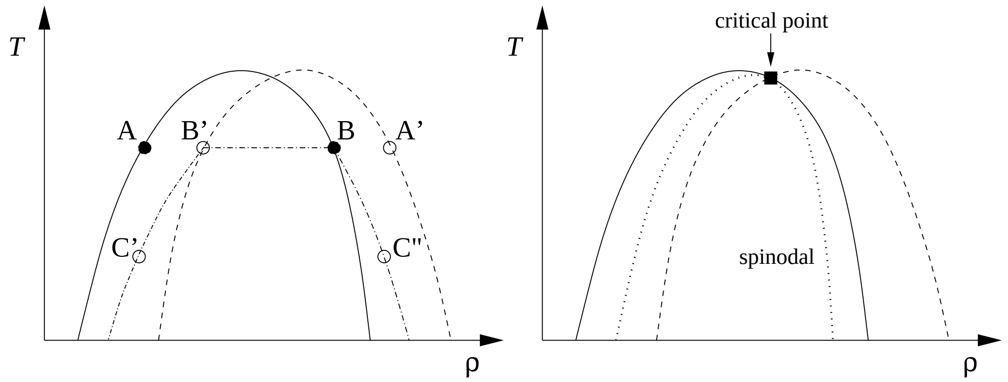

Figure 1: Left: Schematic cloud (solid) and shadow (dashed) curves. On the x-axis is the total particle number density ρ_0. Points A, A' and B, B' form cloud-shadow pairs for the onset of phase coexistence coming from low and high densities, respectively. The dash-dotted lines are coexistence curves for parent B, giving the densities of the two coexisting phases (*e.g.* C', C") into which B separates as temperature is lowered. Right: Schematic spinodal curve (dotted) and critical point.

2.1 Phenomenology of polydisperse phase behaviour

We summarize some important qualitative features of polydisperse phase behaviour. It can be helpful to keep the simple case of a bidisperse system (with two particle species) in mind; for pictorial illustrations of this see *e.g.* [3, 7]. Denote the overall or "parent" density distribution of the system as $\rho^{(0)}(\sigma)$. One can now imagine adding or removing solvent to change the total density $\rho_0^{(0)} = \int d\sigma\, \rho^{(0)}(\sigma)$, while preserving the shape $\rho^{(0)}(\sigma)/\rho_0^{(0)}$ of the distribution. Coming from *e.g.* a low density, single-phase region, the first density where phase separation occurs defines the "cloud point"; there, the parent coexists with an infinitesimal amount of a new "shadow" phase. One can repeat the procedure of finding the onset of phase coexistence for *e.g.* different temperatures; plotting T against the parent (cloud phase) density and the density of the shadow one obtains the cloud curve and shadow curve, respectively (Fig. 1). In a monodisperse system, these two curves would coincide, with a critical point at the maximum. In the polydisperse case, however, the curves are different, and the critical point occurs at their crossing. The reason for this is that the shadow phases will in general have a density distribution $\rho(\sigma)$ with a different shape from that of the parent; they are enriched in some particle species and depleted in others, a process known as "fractionation". Thus, in contrast to a monodisperse system, the roles of cloud and shadow phases cannot be reversed, and cloud and shadow curves are different. That the critical point is located at their crossing (rather than their maximum) follows because at criticality cloud and shadow are by definition identical.

One can also consider spinodals in a polydisperse system; these are the points where a given parent phase first becomes unstable to local density fluctuations. Determining the spinodal densities for *e.g.* a range of temperatures gives a spinodal curve. This lies inside the cloud curve, since outside the cloud curve single phases are stable; the critical point, where the shadow phase can be generated by an infinitesimally small fluctuation, always lies on the spinodal curve and so the spinodal and the cloud curve touch there (see Fig. 1).

Beyond the onset of phase coexistence, polydisperse phase behaviour becomes yet more complex. Tuning *e.g.* temperature past the cloud point, a given parent will separate into two phases neither of which have the original density distribution; only the overall composition across the two phases will be maintained. Plotting T against the total density of the two phases generates two "coexistence" curves that begin on the cloud and shadow curve, respectively (see Fig. 1). Each parent on the dilution line will generate its own set of coexistence curves, all beginning at different points on the cloud and shadow curves.

So far we have only discussed situations where at most two phases coexist. However, in a polydisperse system there is no a priori limit on the number of phases. A possible manifestation of this are kinks in the cloud curve, where the onset of phase separation switches between different branches of two-phase coexistence (*e.g.* separation into a colloidal gas and liquid versus demixing into two colloidal liquids). The shadow curve then exhibits corresponding jumps, reflecting the discontinuous change in the properties of the shadow phase; the kink in the cloud curve is a triple point and marks the beginning of a three-phase coexistence region. Even where the initial phase separation is into two phases, new phases may appear as *e.g.* T is lowered, giving new brances of the coexistence curves.

2.2 Phase equilibria and the moment free energy method

The statistical mechanics of polydisperse systems is also known as "continuous thermodynamics" (see *e.g.* [8]). It is often useful to separate off the ideal part of the free energy (density) explicitly by writing, with the convention $k_{\rm B} = 1$,

$$f([\rho(\sigma)]) = T \int d\sigma\, \rho(\sigma)[\ln \rho(\sigma) - 1] + \tilde{f}([\rho(\sigma)]) \tag{2}$$

This defines the excess free energy $\tilde{f}$. The ideal part is the free energy of an ideal polydisperse gas, which can be got *e.g.* as the limit for $M \to \infty$ of the result for a mixture of M species. From (2), the chemical potentials follow by (functional) differentiation as

$$\mu(\sigma) = \frac{\delta f}{\delta \rho(\sigma)} = T \ln \rho(\sigma) + \tilde{\mu}(\sigma), \qquad \tilde{\mu}(\sigma) = \frac{\delta \tilde{f}}{\delta \rho(\sigma)} \tag{3}$$

and the pressure is given by the Gibbs-Duhem relation

$$\Pi = -f + \int d\sigma\, \mu(\sigma)\rho(\sigma) = T\rho_0 - \tilde{f} + \int d\sigma\, \tilde{\mu}(\sigma)\rho(\sigma) \tag{4}$$

where $\rho_0 = \int d\sigma\, \rho(\sigma)$ is the total number density. In principle, phase splits can be calculated from the conditions of equality of the chemical potentials $\mu(\sigma)$ and the pressure Π between all phases, combined with the requirement of conservation of particle number for each species σ. The latter reads

$$\sum_\alpha v^{(\alpha)} \rho^{(\alpha)}(\sigma) = \rho^{(0)}(\sigma) \tag{5}$$

where, as in (1), $v^{(\alpha)}$ is the fraction of the system volume occupied by phase α. However, since the $\mu(\sigma)$ and Π themselves are functionals of the unknown density distributions

$\rho^{(\alpha)}(\sigma)$ in the coexisting phases, this direct approach is for practical purposes impossible. (Approximations, *e.g.* by splitting the range of σ into discrete bins to recover an effectively finite mixture, are of course possible; see [3] for a survey.)

An important insight came from the seminal work of Gualtieri and others [9, 10]: significant progress can be made for model systems with so-called "truncatable" free energies [4]. These are characterized by an *excess* contribution $\tilde{f} = \tilde{f}(\{\rho_i\})$ that depends only on a finite number, K (say) of generalized *moment densities*

$$\rho_i = \int d\sigma \, w_i(\sigma)\rho(\sigma) \tag{6}$$

of the density distribution $\rho(\sigma)$; for power-law weight functions $w_i(\sigma) = \sigma^i$, the ρ_i are conventional moments. The class of polydisperse colloidal and polymer systems whose (at least approximate) free energies are truncatable is surprisingly large, and includes for example Flory-Huggins theory for homo- and copolymers and van der Waals theories for colloidal gases and liquids [3]; other examples are discussed below.

For a truncatable system, the excess chemical potentials can be written as

$$\tilde{\mu}(\sigma) = \frac{\delta \tilde{f}}{\delta \rho(\sigma)} = \sum_i w_i(\sigma)\tilde{\mu}_i \tag{7}$$

where the $\tilde{\mu}_i = \partial \tilde{f}/\partial \rho_i$ are excess moment chemical potentials. One then finds (see *e.g.* [3]) from equality of the $\mu(\sigma)$, Eq. (3), together with particle conservation (5), that the density distributions in coexisting phases can be written as

$$\rho^{(\alpha)}(\sigma) = \rho^{(0)}(\sigma) \frac{\exp\left[\sum_i \lambda_i^{(\alpha)} w_i(\sigma)\right]}{\sum_\gamma v^{(\gamma)} \exp\left[\sum_i \lambda_i^{(\gamma)} w_i(\sigma)\right]} \tag{8}$$

where the $\lambda_i^{(\alpha)}$ must obey

$$\lambda_i^{(\alpha)} = -\beta\tilde{\mu}_i^{(\alpha)} + c_i \tag{9}$$

(The c_i are undetermined constants that do not affect the density distributions (8); one can fix them *e.g.* by requiring all the $\lambda_i^{(\alpha)}$ in one of the phases to be zero.) A little reflection then shows that (9) together with $\sum_\alpha v^{(\alpha)} = 1$ and the equality of the pressures (4)

$$\Pi = T\rho_0 - \tilde{f} + \sum_i \tilde{\mu}_i \rho_i \tag{10}$$

in all phases give a closed system of nonlinear equations for the $P(K+1)$ variables $\lambda_i^{(\alpha)}$ and $v^{(\alpha)}$: one no longer has to deal with functional equations. A solution can thus, in principle, be found by a standard algorithm such as Newton-Raphson. Generating an initial point from which such an algorithm will converge, however, is still a nontrivial problem, especially when more than two phases coexist and/or many moment densities are involved. Furthermore, the nonlinear phase equilibrium equations permit no simple geometrical interpretation or qualitative insight akin to the construction of phase diagrams from the free energy surface of a finite mixture. To address these two disadvantages, one can construct a "moment free energy" [4, 2, 1]. This takes the crucial reduction from an infinite-dimensional to a finite-dimensional problem from the level of the phase equilibrium conditions to that of the free energy itself.

The starting point is the decomposition (2) for the free energy of truncatable systems

$$f = T\int d\sigma\, \rho(\sigma)\left[\ln\frac{\rho(\sigma)}{R(\sigma)} - 1\right] + \tilde{f}(\{\rho_i\}) \tag{11}$$

In the first (ideal) term, a factor $R(\sigma)$ has been included inside the logarithm. This has no effect on the exact thermodynamics because it contributes only terms linear in $\rho(\sigma)$, but will play a central role below. To motivate the construction of the moment free energy, one can argue that the most important moment densities to treat correctly in the calculation of phase equilibria are those that actually appear in the excess free energy $\tilde{f}(\{\rho_i\})$. Accordingly, one imposes particle conservation (5) only for the ρ_i, but allows it to be violated in other details of the density distribution $\rho(\sigma)$ which do not affect the ρ_i. These "transverse" degrees of freedom are instead chosen to minimize the free energy. Because the excess free energy depends (for a truncatable system) only on the set of moment densities, one therefore has to minimize the ideal part of the free energy (11) over all distributions $\rho(\sigma)$ with fixed moment densities ρ_i. This yields

$$\rho(\sigma) = R(\sigma)\exp\left[\sum_i \lambda_i w_i(\sigma)\right] \tag{12}$$

where the Lagrange multipliers λ_i are chosen to give the desired moment densities

$$\rho_i = \int d\sigma\, w_i(\sigma)\, R(\sigma)\exp\left[\sum_j \lambda_j w_j(\sigma)\right] \tag{13}$$

The corresponding minimum value of f as given in (11) then defines the *moment free energy*

$$f_{\rm mom}(\{\rho_i\}) = T\left(\sum_i \lambda_i\rho_i - \rho_0\right) + \tilde{f}(\{\rho_i\}) \tag{14}$$

Since the Lagrange multipliers are (at least implicitly) functions of the moment densities ρ_i, the moment free energy depends only on the ρ_i. These can now be viewed as densities of "quasi-species" of particles, allowing for example the calculation of "moment chemical potentials" [4]

$$\mu_i = \frac{\partial f_{\rm mom}}{\partial\rho_i} = T\lambda_i + \frac{\partial\tilde{f}}{\partial\rho_i} = T\lambda_i + \tilde{\mu}_i \tag{15}$$

and the corresponding pressure

$$\Pi = \sum_i \mu_i\rho_i - f_{\rm mom} = T\rho_0 + \sum_i \tilde{\mu}_i\rho_i - \tilde{f} \tag{16}$$

which for truncatable systems is identical to the exact expression (10). A finite-dimensional phase diagram can thus be constructed from $f_{\rm mom}$ according to the usual tangency plane rules, ignoring the underlying polydisperse nature of the system. Obviously, though, the results now depend on $R(\sigma)$. To understand its influence, one notes that the moment free energy is simply the free energy of phases in which the density distributions $\rho(\sigma)$ are of the form (12). To ensure that the parent phase is contained in the family, one chooses its density distribution as the prior, $R(\sigma) = \rho^{(0)}(\sigma)$; the moment free energy procedure will then be *exactly valid* whenever the density distributions *actually* *arising* in the various coexisting phases of the system under study *are members of the corresponding family*

$$\rho(\sigma) = \rho^{(0)}(\sigma) \exp\left[\sum_i \lambda_i w_i(\sigma)\right] \tag{17}$$

It is easy to show from (8) that this condition holds whenever all but one of a set of coexisting phases are of infinitesimal volume compared to the majority phase. Accordingly, the moment free energy yields *exact* cloud and shadow curves. Similarly, one can show that spinodals and critical points are found exactly [4]. For coexistences involving finite amounts of different phases the moment free energy only gives approximate results, since different density distributions from the family (17), corresponding to two (or more) phases arising from the same parent $\rho^{(0)}(\sigma)$, do not in general add to recover the parent distribution itself. Moreover, from Gibbs' phase rule, a moment free energy depending on K moment densities will not predict more than $K+1$ coexisting phases, while we know that a polydisperse system can in principle separate into an arbitrary number of phases. Both of these shortcomings can be overcome by including extra moment densities within the moment free energy; this systematically increases the accuracy of any calculated phase splits [4]. By choosing the weight functions of the extra moments adaptively, the properties of the coexisting phases can then be predicted with in principle arbitrary accuracy [11]; the results can even be used as initial points from which a solution of the exact phase equilibrium problem can be converged successfully [12, 13].

In summary, the moment free energy method restores to the problem of polydisperse phase equilibria much of the physical and geometrical insight available from the thermodynamics of finite mixtures. It also leads to computationally efficient procedures which can handle *e.g.* coexistence of more than two phases with relative ease compared to previous approaches; see [3] for an overview.

3 Application I: Hard rods with length polydispersity

Suspensions of anisotropic colloidal particles such as rods can form orientationally ordered phases, *e.g.* nematics which have no long-range translational order, but have rods pointing preferentially along a fixed direction, the nematic axis. For lyotropic systems, whose phase behaviour is controlled primarily by the particle concentration, the simplest and paradigmatic model is that of Onsager [14]. It neglects any long-range attractions between particles and only retains short-range repulsions. The latter are taken to be hard (infinite repulsion on contact); the free energy then has only entropic contributions and temperature becomes an irrelevant scale parameter, set to unity below. Rod-like colloidal particles approximating closely such hard rods can be realized experimentally [15].

Onsager's treatment of the hard rod model is based on a virial expansion in the overall particle density. As is well known, for long thin rods (Onsager limit) and in the region of densities where the I-N phase transition occurs, this expansion truncates after the first nontrivial, *i.e.* second virial, contribution. This makes the model attractive for theoretical study: the free energy is known exactly in terms of the density distribution, even when rod diameters or rod lengths l are polydisperse. That *e.g.* length polydispersity has significant effects on phase behaviour is clear from studies of bi- and tridisperse systems (two/three different rod lengths). For sufficiently disparate lengths coexistence of several nematic phases (N-N), possibly also together with an isotropic phase (I-N-N), is predicted [16, 17, 18, 19, 20, 21] and has been observed experimentally [15]. The N-N

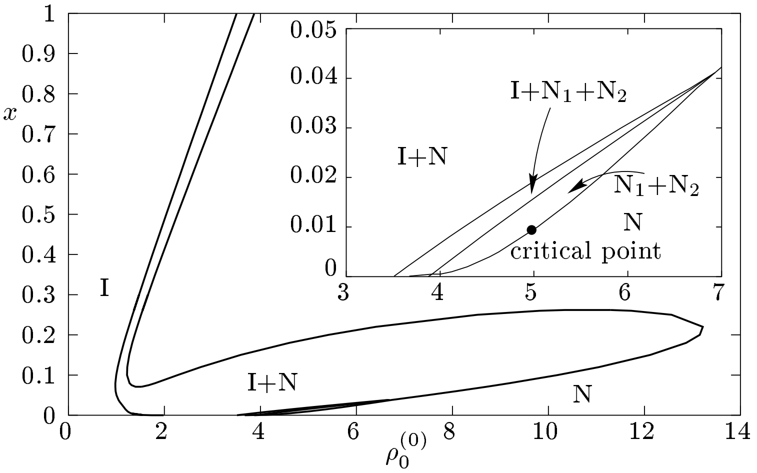

Figure 2: Phase diagram of the P_2-Onsager model with a bimodal length distribution [12]. The rod lengths at the two peaks have the ratio 12; x is the fraction of long rods; $\rho_0^{(0)}$ is the parent number density. Only phase boundaries are shown; the lines separating one- and two-phase regions are cloud curves. The small I-N-N coexistence region is expanded in the inset; towards very small x (not visible) it is bordered by an I-N region. For larger x, the I-N phase boundary is re-entrant.

region in the bidisperse phase diagram is terminated by a critical point for length ratios between around 2.9 and 3.2 [22] but is open towards large densities [18, 19, 20] for larger ratios. Re-entrant phase coexistence sequences such as I $\to$ I-N $\to$ N $\to$ I-N $\to$ N have also been found [16]. More quantitative effects of polydispersity include a broadening of the I-N coexistence region and fractionation of longer rods into the nematic; these are also found in perturbative treatments [23, 24] for small normalized width (often also referred to as polydispersity) $s = (\langle l^2 \rangle - \langle l \rangle^2)/\langle l \rangle^2$ of the length distribution.

Understanding the phase behaviour of the Onsager theory for a continuous length distribution with non-infinitesimal width s has until recently remained an open problem. No simple inferences are possible from the results for the bi- or tridisperse cases; otherwise one would incorrectly predict, for example, that *any* polydisperse system should show N-N coexistence since it contains *some* rods of very different lengths. Tackling the full polydisperse Onsager theory head on is, however, difficult for two reasons. Firstly, the relevant density distribution $\rho(l, \theta)$ depends both on the conserved rod lengths l and the non-conserved angles θ which the rods make with the nematic axis. Fortunately, the moment method can be extended to this more complex situation [11]. Second, the full Onsager theory is not truncatable: its excess (second virial) free energy involves an infinite number of moment densities defined by the weight functions $lP_{2n}(\cos\theta)$, where the P_{2n} are Legendre polynomials [25]. We therefore first studied the Zwanzig model of rods oriented along one of three perpendicular axes. Within a second virial approximation this has a truncatable excess free energy, so that the fully length-polydisperse case can be treated [11]. The results confirm the general trends towards broadening of the I-N region and stronger fractionation with increasing polydispersity s. However, no evidence for N-N coexistence was found, even for large s; this can be traced back to the model's underestimate of the gain in orientational entropy on N-N demixing [3].

To avoid this effect, we next studied a version of the Onsager model with continuous rod orientations, obtained by truncating the Legendre polynomial expansion after the

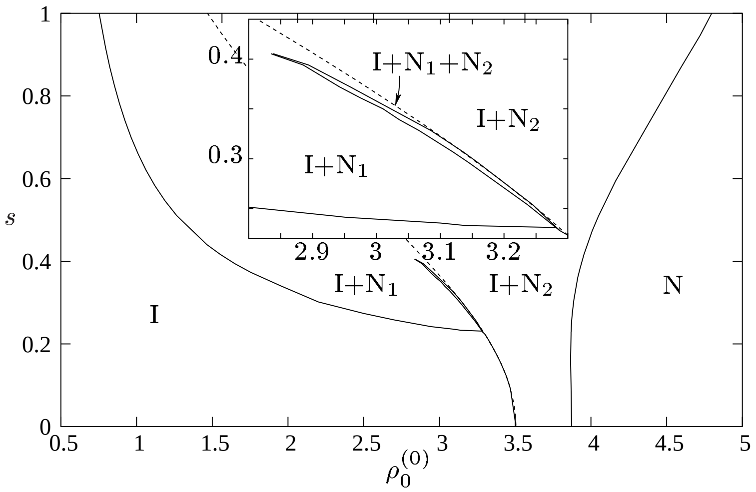

Figure 3: As Fig. 2, but with a lognormal length distribution (cut off at $100\times$ the average rod length [13]). The y-axis shows the polydispersity s, *i.e.* the normalized width of the distribution. Note the difference in topology to Fig. 2: the narrow I-N-N region is now fully surrounded by the I-N coexistence region and does not connect to an N-N region at higher densities. The dashed line gives the I-N phase boundary for a generic (here: Schulz) length distribution which does not have a fat tail; the presence of very long rods in the lognormal distribution causes a strong broadening of the coexistence region.

first nontrivial term [12]. The resulting "P_2-Onsager model" does indeed exhibit I-N-N and N-N coexistence for appropriate bidisperse and bimodal (double-peaked) distributions of rod lengths; see Fig. 2. The results suggested that this behaviour could be generic whenever the system contained a sufficient (but not too large) number of rods that were substantially longer than the average. A Schulz-Gamma distribution of rod lengths $P(l) \propto l^z \exp[-(z+1)l]$ was found not to have enough of a "fat tail" of long rods for this condition to be met. A lognormal distribution, however, does [13], providing an example where even a length distribution with a single peak produces I-N-N coexistence (Fig. 3).

Most recently, we have developed a numerical algorithm to solve for the onset of I-N coexistence in the full, untruncated Onsager theory with polydispersity [26]. With a lognormal length distribution, kinks again appear in the cloud curve; even though we cannot calculate three-phase I-N-N equilibria explicitly at present, these kinks demonstrate that an I-N-N coexistence region must exist in the phase diagram. More surprisingly when compared to the results of the approximate P_2 model, even a Schulz distribution shows this effect: above a threshold value $s = 1/2$ of the polydispersity, the longest rods in the system have an effect seemingly out of all proportion with their exponentially small concentration, and in fact dominate the rod length distribution in the nematic shadow phase. The Onsager theory seems to be the first model where the incorporation of seemingly "innocent" polydispersity (via an exponential tail of longer rods) has such drastic effects.

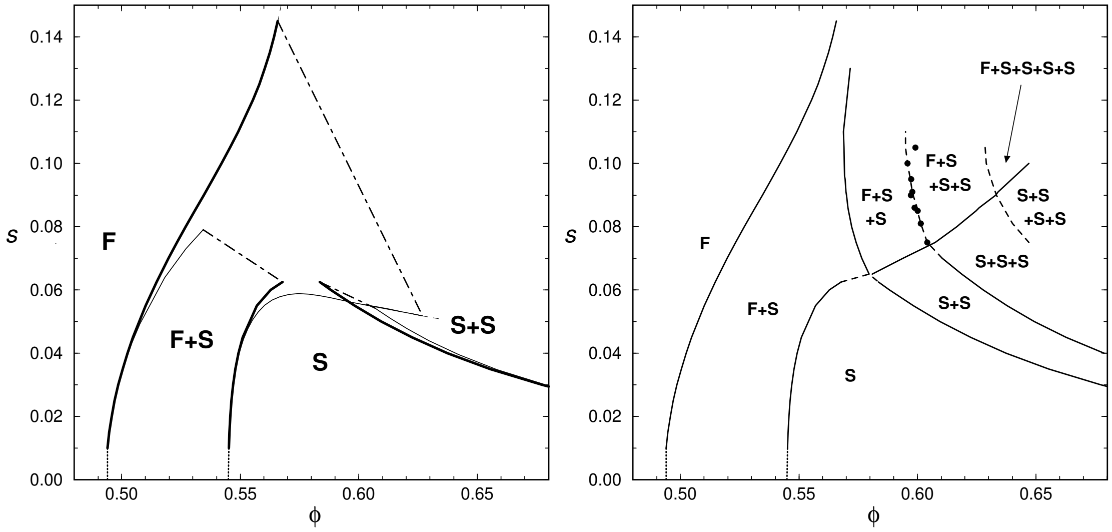

Figure 4: Left: Cloud (thick) and shadow (thin) curves for polydisperse hard spheres with a triangular diameter distribution. Volume fraction ϕ and polydispersity s are shown; dash-dotted lines link exemplary cloud-shadow pairs. The fluid (F) cloud curve continues to relatively large s; the coexisting shadow solid has smaller s below $\approx 6\%$. The solid (S) cloud curve has two branches: onset of F-S and S-S coexistence on the left and right, respectively. Right: Corresponding phase diagram, showing the various phase coexistences beyond the cloud curves. At higher ϕ and s, multiple solid coexistence can occurs, also with a fluid. Dashed lines are phase boundaries drawn by hand on the basis of preliminary data; note in particular that the two branches of the solid cloud curve must meet.

4 Application II: Polydisperse hard spheres

As a second application we consider the phase behaviour of suspensions of spherical colloids with polydispersity in size (diameter σ); again we focus on the simplest case of only hard repulsion. This can be realized experimentally, using for example latex particles sterically stabilized by a polymer coating [27]. Monodisperse hard spheres exhibit only a freezing transition, with a fluid of volume fraction $\phi \approx 50\%$ coexisting with a crystalline solid with $\phi \approx 55\%$. It was suggested early on that diameter polydispersity might destabilize the crystal phase and inhibit freezing above some "terminal" polydispersity s_t. Experiments support this notion [27], but the situation is somewhat ambiguous since a kinetic glass transition [28] might intervene; the growth kinetics of polydisperse crystals could also cause deviations from equilibrium behaviour [29]. We nevertheless focus here on the equilibrium phase diagram of polydisperse hard spheres, which will certainly be required as a baseline from which to establish the importance of non-equilibrium effects.

Much early theoretical work (see [3, 30] for references) focussed on estimating s_t. Computer simulations have also been used (*e.g.* [31]), but are conventionally carried out at constant chemical potentials $\mu(\sigma)$. In contrast to the experimental situation, the parent density distribution $\rho^{(0)}(\sigma)$ can then change shape dramatically across the calculated phase diagram. Recent work has addressed this problem [32], but has not yet been extended to the calculation of phase equilibria.

To investigate the phase behaviour systematically, one needs appropriate free energy expressions for the fluid and solid. For the fluid, the most accurate approximation available at present is the BMCSL generalization [33, 34] of the monodisperse Carnahan-Starling equation of state. This corresponds to a truncatable excess free energy [6] involving four moment densities (σ^i, $i = 0 \ldots 3$). For the crystalline solid, Bartlett [35, 36] proposed to *assume* that such a moment structure again exists; an approximate excess free energy can then be derived from simulation data for bidisperse hard sphere systems. We have very recently performed accurate phase diagram calculations with these free energies; approximate results had earlier been obtained by Bartlett and Warren [37]. They found that the range of volume fractions where fluid-solid coexistence is observed narrows as the polydispersity s is increased and eventually shrinks to zero at a terminal polydispersity $s_t \approx 8\%$. At values of s just below s_t, they also found a transition to a re-entrant fluid at large volume fractions.

However, the approximations in [37] constrained the polydispersity s to be equal in the fluids and solid, disallowing the physically plausible possibility of a polydisperse fluid splitting off a solid with a narrower size distribution. Without this approximation, our calculations show that the fluid cloud curve indeed continues to larger s, while the coexisting solid shadow phase never exceeds polydispersities of $s \approx 6\%$ (Fig. 4). In this sense, the terminal polydispersity only exists for the solid (see also [38]); fluids with $s >$ 6% *can* crystallize but only by producing a fractionated solid with a narrower range of particle sizes. Because of this, the point of equal concentration found in [37] disappears. The predicted re-entrant melting is also modified: instead of returning to fluid-solid coexistence and eventually a single-phase fluid at high volume fractions, a polydisperse solid splits into two fractionated solids. At sufficiently large s, a larger number of solid phases can occur, consistent with the simplified calculations of [35]; coexistence of several solids with a fluid phase is also possible. Our calculated phase diagram (Fig. 4) thus unites and clarifies the previous separate predictions of polydispersity effects on fluid-solid coexistence and solid-solid fractionation. An additional feature not shown in Fig. 4 is fluid-fluid demixing; this has been predicted for polydisperse systems [39, 40] but with polydispersities s of order 100%, far outside the displayed range.

5 Conclusion

We have given an overview of polydisperse phase behaviour, focussing on theoretical prediction of bulk phase coexistence. Polydisperse systems are characterized by an effectively infinite number of distinguishable particle species, and thus conserved densities, and this makes the task of predicting phase equilibria from a known free energy highly nontrivial. A reduction to a finite-dimensional problem is essential; this can be achieved using the moment free energy method, which restores much geometrical insight by expressing the free energy in terms of the densities of a finite number of "quasi-species". The method can be applied to all truncatable models, *i.e.* those whose excess free energy depends only on a number of moments of the density distribution. We gave exemplary results for suspensions of colloidal hard rods with length polydispersity, and for polydisperse hard spherical colloids. The phase behaviour that even these relatively simple models produce is extremely rich compared to that of monodisperse systems, and many intriguing questions remain unanswered in the field. As surveyed in [3], the same is true to an even greater degree of the largely unexplored areas of interfacial behaviour and phase separation kinetics in polydisperse systems.

Acknowledgements: MF and PS acknowledge financial support through EPSRC grant GR/R52121/01.

References

[1] P. Sollich and M. E. Cates, Phys. Rev. Lett. **80**, 1365 (1998).

[2] P. B. Warren, Phys. Rev. Lett. **80**, 1369 (1998).

[3] P. Sollich, J. Phys. Cond. Matt. **14**, R79 (2002).

[4] P. Sollich, P. B. Warren, and M. E. Cates, Adv. Chem. Phys. **116**, 265 (2001).

[5] R. T. DeHoff, *Thermodynamics in Material Science* (McGraw-Hill, New York, 1992).

[6] J. J. Salacuse and G. Stell, J. Chem. Phys. **77**, 3714 (1982).

[7] R. Koningsveld, Pure Appl. Chem. **20**, 271 (1969).

[8] M. T. Rätzsch and C. Wohlfarth, Adv. Polymer Sci. **98**, 49 (1991).

[9] J. A. Gualtieri, J. M. Kincaid, and G. Morrison, J. Chem. Phys. **77**, 521 (1982).

[10] E. M. Hendriks, Fluid Phase Eq. **33**, 207 (1987).

[11] N. Clarke *et al.*, J. Chem. Phys. **113**, 5817 (2000).

[12] A. Speranza and P. Sollich, J. Chem. Phys. **117**, 5421 (2002).

[13] A. Speranza and P. Sollich, (2002), preprint cond-mat/0208193.

[14] L. Onsager, Ann. N.Y. Acad. Sci. **51**, 627 (1949).

[15] P. A. Buining and H. N. W. Lekkerkerker, J. Phys. Chem. **97**, 11510 (1993).

[16] H. N. W. Lekkerkerker, P. Coulon, R. van der Haegen, and R. Deblieck, J. Chem. Phys. **80**, 3427 (1984).

[17] T. Odijk and H. N. W. Lekkerkerker, J. Phys. Chem. **89**, 2090 (1985).

[18] G. J. Vroege and H. N. W. Lekkerkerker, J. Phys. Chem. **97**, 3601 (1993).

[19] R. van Roij and B. Mulder, J. Chem. Phys. **105**, 11237 (1996).

[20] G. J. Vroege and H. N. W. Lekkerkerker, Colloids Surf. A **130**, 405 (1997).

[21] P. C. Hemmer, Molecular Physics **96**, 1153 (1999).

[22] S. Varga and I. Szalai, Phys. Chem. Chem. Phys. **2**, 1955 (2000).

[23] T. J. Sluckin, Liquid Crystals **6**, 111 (1989).

[24] Z. Y. Chen, Phys. Rev. E **50**, 2849 (1994).

[25] R. F. Kayser and H. J. Raveche, Phys. Rev. A **17**, 2067 (1978).

[26] A. Speranza and P. Sollich, (2002), preprint cond-mat/0211103.

[27] P. N. Pusey and W. van Megen, Nature **320**, 340 (1986).

[28] P. N. Pusey and W. van Megen, Phys. Rev. Lett. **59**, 2083 (1987).

[29] R. M. L. Evans and C. B. Holmes, Phys. Rev. E **64**, 011404 (2001).

[30] S. E. Phan, W. B. Russel, J. X. Zhu, and P. M. Chaikin, J. Chem. Phys. **108**, 9789 (1998).

[31] P. G. Bolhuis and D. A. Kofke, Phys. Rev. E **54**, 634 (1996).

[32] N. B. Wilding and P. Sollich, J. Chem. Phys. **116**, 7116 (2002).

[33] T. Boublik, J. Chem. Phys. **53**, 471 (1970).

[34] G. A. Mansoori, N. F. Carnahan, K. E. Starling, and T. W. Leland, Jr., J. Chem. Phys. **54**, 1523 (1971).

[35] P. Bartlett, Mol. Phys. **97**, 685 (1999).

[36] P. Bartlett, J. Chem. Phys. **107**, 188 (1997).

[37] P. Bartlett and P. B. Warren, Phys. Rev. Lett. **82**, 1979 (1999).

[38] D. A. Kofke and P. G. Bolhuis, Phys. Rev. E **59**, 618 (1999).

[39] P. B. Warren, Europhys. Lett. **46**, 295 (1999).

[40] J. A. Cuesta, Europhys. Lett. **46**, 197 (1999).